

Atomic parity nonconservation and neutron radii in cesium isotopes

B. Q. Chen

W. K. Kellogg Radiation Laboratory, 106-38, California Institute of Technology, Pasadena, California 91125

P. Vogel

Norman Bridge Laboratory of Physics, 161-33, California Institute of Technology, Pasadena, California 91125

(Received 5 March 1993)

The interpretation of future precise experiments on atomic parity violation in terms of parameters of the standard model could be hampered by uncertainties in the atomic and nuclear structure. While the former can be overcome by measurement in a series of isotopes, the nuclear structure requires knowledge of the neutron density. We use the nuclear Hartree-Fock method, which includes deformation effects, to calculate the proton and neutron densities in ^{125}Cs – ^{139}Cs . We argue that the good agreement with the experimental charge radii, binding energies, and ground-state spins signifies that the phenomenological nuclear force and the method of calculation that we use is adequate. Based on this agreement, and on calculations involving different effective interactions, we estimate the uncertainties in the differences of the neutron radii $\delta\langle r^2 \rangle_{N,N'}$ and conclude that they cause uncertainties in the ratio of weak charges, the quantities determined in the atomic parity nonconservation experiments, of less than 10^{-3} . Such an uncertainty, although to some extent model dependent, is safely smaller than the anticipated experimental error.

PACS number(s): 21.10.Gv, 21.60.Jz, 12.15.Ji

I. INTRODUCTION

Precision studies of electroweak phenomena provide very important tests of the $\text{SU}(2)_L \times \text{U}(1)$ standard electroweak model. The measurement of the parity nonconserving (PNC) components of the atomic transitions belongs to this class. It offers a unique opportunity for testing the electroweak radiative corrections at the one loop level and, possibly, to search for new physics beyond the standard model [1,2].

The PNC effects in atoms are caused by γ, Z^0 interference in the electron-nucleus interaction. The dominant contribution comes from the coupling of the axial electronic current to the vector nuclear current. (The interaction of the electronic vector current with the nuclear axial current is weaker in heavy atoms, and can be eliminated by summing over the PNC effects in the resolved hyperfine components of the atomic transitions. The hyperfine-dependent effect, which also includes the nuclear anapole moment, is of interest in its own right [3,4], but is not considered hereafter.) Since the vector current is conserved, atomic PNC essentially measures the electroweak coupling of the elementary quarks.

At the present time, PNC measurements in stable ^{133}Cs atoms have $\pm 2\%$ experimental uncertainty [5]. (An earlier experiment in Cs was performed by Bouchiat *et al.* [6]; the studies of PNC effects in atoms have been reviewed by Commins [7] and Telegdi [8].) However, improvement by an order of magnitude in the experimental accuracy is anticipated and a possibility of measuring PNC effects in unstable cesium and francium isotopes has been discussed [9]. At this level, two issues must be resolved before an interpretation of the PNC data in terms of the fundamental electroweak couplings is possi-

ble. The atomic theory, even in its presently most sophisticated form [10,11], introduces about $\pm 1\%$ uncertainty. Moreover, the small but non-negligible effects of nuclear size [12,13] must be addressed. This latter problem is the main topic of the present work.

Atomic PNC is governed by the effective bound electron-nucleus interaction (when taking only the part that remains after averaging over the hyperfine components) of the form

$$H_{\text{PNC}} = \frac{G_F}{2\sqrt{2}} \int [-N\rho_n(\mathbf{r}) + Z(1 - 4\sin^2\theta_W)\rho_p(\mathbf{r})] \times \psi_e^\dagger \gamma_5 \psi_e d^3r, \quad (1)$$

where the proton and neutron densities $\rho_{p,n}(\mathbf{r})$ are normalized to unity, and we have assumed the standard model nucleon couplings

$$C_{1p} \equiv 2C_{1u} + C_{1d} = \frac{1}{2}(1 - 4\sin^2\theta_W), \quad (2)$$

$$C_{1n} \equiv C_{1d} + 2C_{1u} = -\frac{1}{2}. \quad (3)$$

The electron part in Eq. (1) can be parametrized as [12,13]

$$\rho_5(r) \equiv \psi_p^\dagger \gamma_5 \psi_s = C(Z)\mathcal{N}(Z,R)f(r), \quad (4)$$

where $C(Z)$ contains all atomic-structure effects for a point nucleus, \mathcal{N} is a precisely calculable normalization factor, and $f(r)$ describes the spatial variation [normalized such that $f(0) = 1$]. It is the integrals

$$q_{n,p} = \int f(r)\rho_{p,n}(\mathbf{r})d^3r \quad (5)$$

that determine the effect of the proton and neutron distributions on the PNC observables.

The form factors $f(r)$ can be calculated to the order $(Z\alpha)^2$ for a sharp nuclear surface of radius R , and neglecting the electron mass in comparison with the nuclear Coulomb potential [12,13],

$$f(r) \simeq 1 - \frac{1}{2}(Z\alpha)^2[(r/R)^2 - \frac{1}{5}(r/R)^4 + \frac{1}{75}(r/R)^6]. \quad (6)$$

For accurate calculations numerical evaluation of $f(r)$ is necessary (see below). However, the coefficients at $\langle r^2 \rangle$ and $\langle r^4 \rangle$ remain numerically of the order $(Z\alpha)^2$ and depend only weakly on the exact shape of $\rho_{p,n}(\mathbf{r})$. In addition, since the electric potential near the nucleus is very strong, one can safely neglect atomic binding energies in the evaluation of $f(r)$ (but not the electron mass). Below we will separate the effects of the finite nuclear size (i.e., effects related to the deviations of $q_{n,p}$ from unity); these terms will be represented by a nuclear-structure correction to the weak charge.

Taking the matrix element of H_{PNC} , one obtains

$$\langle i | H_{\text{PNC}} | j \rangle = \frac{G_F}{2\sqrt{2}} C(Z) \mathcal{N} [Q_W(N, Z) + Q_W^{\text{nuc}}(N, Z)], \quad (7)$$

where $Q_W(N, Z)$, the quantity of primary interest from the point of view of testing the standard model, is the “weak charge.” In the standard model, with couplings (2) and (3), the weak charge is

$$Q_W = -N + Z(1 - 4 \sin^2 \theta_W). \quad (8)$$

The nuclear-structure correction $Q_W^{\text{nuc}}(N, Z)$ describes the part of the PNC effect that is caused by the finite nuclear size. In the same approximation as Eq. (8) above,

$$Q_W^{\text{nuc}} = -N(q_n - 1) + Z(1 - 4 \sin^2 \theta_W)(q_p - 1), \quad (9)$$

where $q_{n,p}$ are the integrals of $f(r)$ defined above. (Nuclear structure also affects the normalization factor \mathcal{N} , which is, however, determined by the known nuclear charge distribution [12,13].)

In a measurement that involves several isotopes of the same element, ratios of the PNC effects depend essentially only on the ratio of the weak charges and the corresponding nuclear-structure corrections $Q_W(N, Z) + Q_W^{\text{nuc}}(N, Z)$. (The dependence \mathcal{N} on the neutron number N will not be considered here.) The ratios of the nuclear-structure-corrected weak charges, in turn, depend, to a good approximation, only on the differences Δq_n of the neutron distributions in the corresponding isotopes. The uncertainties in these quantities, or equivalently, in the differences of the neutron mean square radii $\delta(\Delta \langle r^2 \rangle_{N, N'})$, then ultimately limit the accuracy with which the fundamental parameters, such as $\sin^2 \theta_W$, can be determined.

It is the purpose of this work to evaluate quantities $q_{n,p}$ for a number of cesium isotopes which might be used in future high-precision PNC experiments [9]. Moreover, we estimate the uncertainty in these quantities, respectively, in their differences, since they represent the ultimate lim-

itations for the interpretation of the PNC measurements.

In Sec. II we describe the nuclear Hartree-Fock calculations that we performed. In Sec. III we compare the calculated binding energies, ground state spins, and charge radii with the experiment. There we also discuss how corrections for the zero-point vibrational motion can be estimated and added. From the spread between the results obtained with two different successful effective Skyrme forces, and from the pattern of deviations between the calculated and measured isotope shifts in the charge radii, we then estimate the uncertainties in the corresponding differences of the neutron radii. Finally, in Sec. IV, we calculate the nuclear-structure corrections to the weak charges, $Q_W^{\text{nuc}}(Z = 55, N = 72-84)$, and their uncertainties and discuss the corresponding limiting uncertainties in the determination of the fundamental parameters of the standard model. [Our notation follows that of Ref. [13]. Others, e.g., Ref. [10], do not explicitly separate the nuclear-structure-dependent effects. We believe that such a separation is very useful, since, as stated above, $f(r)$ in Eq. (6) and hence also $q_{n,p}$, Eq. (5), are essentially independent of atomic structure.]

II. NUCLEAR HARTREE-FOCK CALCULATION

As demonstrated by numerous calculations, the microscopic description of nuclear ground state properties by means of the Hartree-Fock (HF) method with an effective Skyrme-like force interaction has been remarkably successful [14,15]. The few adjustable parameters in the Skyrme force are chosen to fit the various bulk properties (energy per nucleon, compressibility modulus, symmetry energy, etc.), and properties of several doubly magic nuclei (binding energies, charge radii, etc.) [16]. The two most popular sets of Skyrme parameters, namely, Skyrme III and SkyrmeM* have been successfully employed to describe the properties of nuclei in several regions of the periodic table [17,18]. Below we show only a few formulas essential to a basic understanding of the numerical calculation that we performed; details can be found in the quoted references.

The generalized Skyrme force (including all possible spin-exchange terms and zero-range density-dependent interaction) can be written as

$$\begin{aligned} V_s = & t_0(1 + x_0 P_\sigma) \delta + \frac{1}{2} t_1(1 + x_1 P_\sigma) (\mathbf{k}^2 \delta + \delta \mathbf{k}'^2) \\ & + t_2(1 + x_2) P_\sigma \mathbf{k} \cdot \delta \mathbf{k}' \\ & + \frac{1}{6} t_3 \rho^\alpha \delta + iW(\boldsymbol{\sigma}_1 + \boldsymbol{\sigma}_2) \cdot \mathbf{k} \times \delta \mathbf{k}', \end{aligned} \quad (10)$$

where t_{0-3} , x_{0-2} , and W are the adjustable parameters, and $\delta \equiv \delta(\mathbf{r} - \mathbf{r}')$.

Because we are dealing with odd- A nuclei, the unpaired nucleon introduces terms that break time-reversal symmetry in the HF functional. When the spin degrees of freedom are taken into account, the breaking of time-reversal symmetry leads to a rather complicated functional [19,20]. The total energy E , which is minimized in the HF method, can be written as a space integral of a local energy density,

$$E = \int \mathcal{H}(\mathbf{r}) d^3 \mathbf{r}, \quad (11)$$

with

$$\begin{aligned}
\mathcal{H}(\mathbf{r}) = & \frac{\hbar^2}{2m} \tau + B_1 \rho^2 + B_2(\rho_n^2 + \rho_p^2) + B_3(\rho\tau - \mathbf{j}^2) + B_4(\rho_n\tau_n - \mathbf{j}_n^2 + \rho_p\tau_p - \mathbf{j}_p^2) \\
& + B_5\rho\Delta\rho + B_6(\rho_n\Delta\rho_n + \rho_p\Delta\rho_p) + B_7\rho^{2+\alpha} + B_8\rho^\alpha(\rho_n^2 + \rho_p^2) \\
& + B_9(\rho\nabla \cdot \mathbf{J} + \mathbf{j} \cdot \nabla \times \boldsymbol{\rho} + \rho_n\nabla \cdot \mathbf{J}_n + \mathbf{j}_n \cdot \nabla \times \boldsymbol{\rho}_n + \rho_p\nabla \cdot \mathbf{J}_p + \mathbf{j}_p \cdot \nabla \times \boldsymbol{\rho}_p) \\
& + B_{10}\rho^2 + B_{11}(\rho_n^2 + \rho_p^2) + B_{12}\rho^\alpha\rho^2 + B_{13}\rho^\alpha(\rho_n^2 + \rho_p^2) + E_C.
\end{aligned} \tag{12}$$

For complete expressions of the Coulomb energy E_C and the coefficients B_i ($i = 1, \dots, 13$), see Ref. [20], where the dependence on Skyrme force parameters in Eq. (10) is given. The mass densities ρ_τ , kinetic density τ_τ , current density \mathbf{j}_τ , spin-orbit density $\nabla \cdot \mathbf{J}_\tau$, and vector density $\boldsymbol{\rho}_\tau$ ($\tau = n, p$) in Eq. (12) can, in turn, be expressed in terms of the single-particle wave functions Φ_k . The variation of E with respect to $\Phi_k^*(\mathbf{r}, \sigma)$ defines the one-body Hartree-Fock Hamiltonian h [20].

In the following we will use the mass densities ρ_τ , which can be expressed as

$$\rho(\mathbf{r}) = \sum_{k,\sigma} v_k^2 |\Phi_k(\mathbf{r}, \sigma)|^2. \tag{13}$$

Here $\Phi_k(\mathbf{r}, \sigma)$ denotes the component of the k th single-nucleon wave function with spin $\frac{1}{2}\sigma$ ($\sigma = \pm 1$) along the z direction, and v_k^2 are the BCS occupation factors (see below). The expressions for the other densities are again given in Ref. [20].

The mean square proton and neutron radii are given by the usual formulas

$$r_\tau^2 = \int r^2 \rho_\tau(\mathbf{r}) d^3\mathbf{r}. \tag{14}$$

In this work, two discrete symmetries, namely, parity and z signature, are imposed on the wave functions [15,20]. The complete description of a wave function requires four real functions corresponding to the real, imaginary, spin-up, and spin-down parts of Φ_k [20].

The numerical approximation to the HF energy E is obtained by a discretization of the configuration space on a three-dimensional rectangular mesh. The mesh size Δx is the same in the three directions and the abscissas of the mesh points are $\frac{1}{2}(2n+1)\Delta x$. In this work, Δx is 0.8 fm, and the mesh size is $16 \times 16 \times 16$. The numerical procedure is described in detail in Ref. [15].

Pairing correlations need to be included in a realistic description of medium and heavy nuclei. We choose to describe pairing between identical nucleons within the BCS formalism using a constant strength seniority force [15]. In the usual BCS scheme, the paired states are assumed to be the two time-reversed orbitals Φ_k and $\Phi_{\bar{k}}$. Although time-reversal symmetry is broken in our calculations of odd- A nuclei, the time-reversal breaking terms in the functional generated by the unpaired odd nucleon are very small compared to the time-reversal conserving terms so that the time-reversal symmetry is still approximately good. In our calculation we define the pairing partner $\Phi_{\bar{k}}$ of state Φ_k to be the eigenstate of h whose overlap with $\hat{T}\Phi_k$ is maximal (\hat{T} is the time-reversal operator). Because the single-particle orbital occupied by the unpaired nucleon and its signature partner do not

contribute to the pairing energy, we introduce blocking in our code to prevent these two orbitals from participating in pairing and force their BCS occupation numbers to be 1 and 0, respectively.

In the following calculations, the proton and neutron BCS pairing strengths are chosen to be 17.5/(11 + Z) MeV and 16.5/(11 + N) MeV, respectively. Although the pairing strengths do affect the binding energies, they have little influence on the neutron or proton radii.

As some of the cesium isotopes considered here are deformed, it is very important to take the deformation degrees of freedom into account. The method of solving the HF+BCS equations by discretization of the wave functions on a rectangular mesh allows any type of even multipole deformation. The deformation energy curves are obtained by a constraint on the mass quadrupole tensor $Q_{ij} = (3x_i x_j - r^2 \delta_{ij})$. The two discrete symmetries of the wave functions Φ_k ensure that the principal axes of inertia lie along the coordinate axes. The quadrupole tensor is, therefore, diagonal and its principal values Q_i can be expressed in terms of two quantities Q_0 and γ as

$$Q_i = Q_0 \cos(\gamma + i\frac{2}{3}\pi), \quad i = 1, 2, 3, \tag{15}$$

where Q_0 and γ satisfy the inequalities

$$Q_0 \geq 0, \quad 0 \leq \gamma \leq \frac{2}{3}\pi. \tag{16}$$

The values of the three constraints Q_i were computed from the desired values of Q_0 and γ and inserted in a quadratic constraint functional added to the variational energy, according to the method described in Ref. [21]. In the calculations described below, we constrain the nuclear shape to be axially symmetric ($\gamma = 0$).

III. COMPARISON WITH EXPERIMENT

In Fig. 1 we show the potential energy curves for ^{125}Cs – ^{139}Cs . According to our calculations with SkyrmeIII (SkmIII) and SkyrmeM* (SkM*) forces the lighter cesium isotopes $N \leq 76$ are deformed. For SkmIII such an assignment is able to explain the observed ground state spins of $\frac{1}{2}^+$ for $N = 70$ – 74 and $\frac{5}{2}^+$ for $N = 76$. For SkM* the mean field proton states $g_{7/2}$ and $d_{5/2}$ are interchanged and therefore the ground state spin assignments for the deformed cesium isotopes are not correct. (This turns out not to be a very crucial problem.) Binding energies and shifts $\delta r_{p,n}^2$ and $\delta r_{p,n}^4$ calculated with the SkM* and SkmIII interactions are shown in Tables I and II. The binding energies agree in both cases with the experimental values with largest deviation of 4 MeV out of about 1000 MeV of total binding energy.

The comparison between the measured and calculated isotope shifts is illustrated in Figs. 2 and 3 as a series

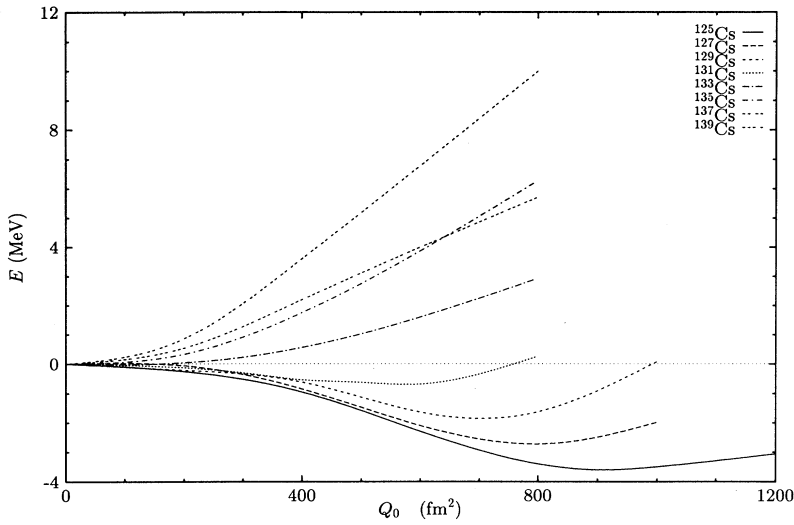


FIG. 1. The potential energy curves for the isotopes ^{125}Cs – ^{139}Cs calculated by the Hartree-Fock method using the SkmIII interaction. The notations are shown on the figure.

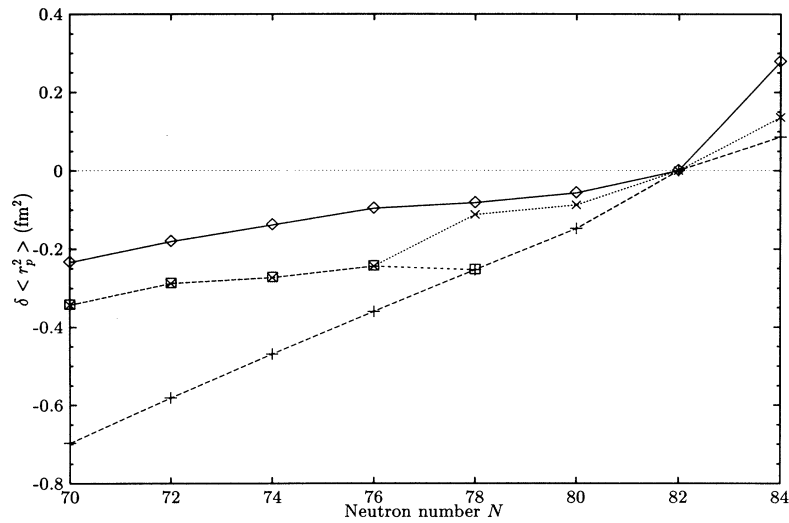


FIG. 2. Calculated and experimental isotope shifts $\delta\langle r_p^2 \rangle$ in cesium, normalized to the semimagic ^{137}Cs . The SkM* interaction has been used. The correction for zero-point vibrations is described in the text. The following notations are used: experimental isotope shift \diamond , spherical HF isotope shifts $+$, HF including equilibrium deformation \square , and corrected for zero-point vibrations \times .

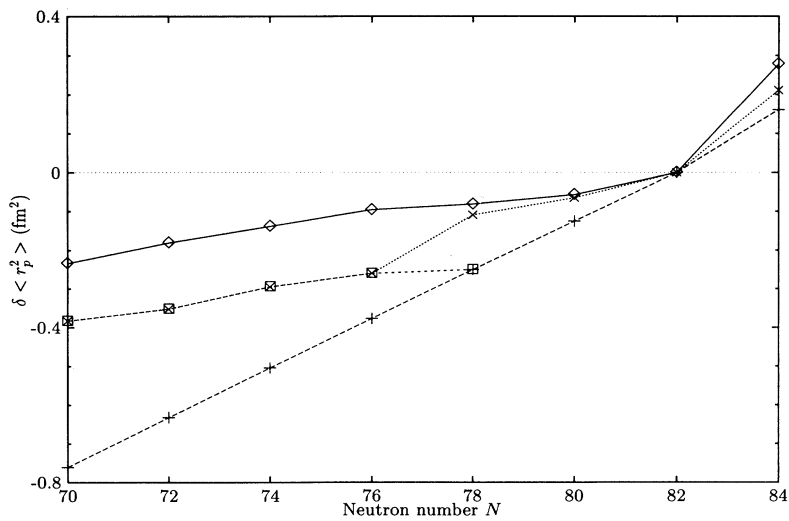


FIG. 3. Calculated and experimental isotope shifts $\delta\langle r_p^2 \rangle$ in cesium. The SkmIII interaction has been used. The correction for zero-point vibrations is described in the text. The same notations used in Fig. 2 are used here.

TABLE I. Results of the Hartree-Fock calculations with the SkM* interactions. The experimental binding energies and isotope shifts $\delta\langle r_p^2 \rangle$ are also listed for comparison. (The binding energies are in MeV, all radial moments in fm.) The experimental isotope shifts are from Ref. [32], normalized to the stable isotope ^{133}Cs .

N	B	B_{HF}	$\delta r_p^2(\text{expt})$	δr_p^2	$\delta r_p^2(\text{sph.})$	δr_p^4	δr_n^2	$\delta r_n^2(\text{sph.})$	δr_n^4
70	1049.98	1045.82	-0.1517	-0.0899	-0.4445	7.987	-0.6803	-1.0787	-31.126
72	1068.25	1064.38	-0.0985	-0.0348	-0.3285	8.836	-0.4603	-0.7931	-19.563
74	1085.66	1082.15	-0.0561	-0.0199	-0.2161	6.247	-0.2927	-0.5186	-11.931
76	1102.37	1099.36	-0.0141	0.0090	-0.1070	4.306	-0.1253	-0.2544	-4.538
78	1118.52	1117.69	0.0000	0.0000	0.0000	0.000	0.0000	0.0000	0.000
80	1134.24	1135.71	0.0250	0.1054	0.1054	4.872	0.2454	0.2454	14.025
82	1149.27	1152.18	0.0821	0.2531	0.2531	9.658	0.5132	0.5132	28.754
84	1159.57	1164.16	0.3604	0.3394	0.3394	17.820	0.8866	0.8866	59.902

of successively better approximations. First, the crosses, connected by dashed lines to guide eyes, show the isotope shifts for spherical nuclei. The agreement with experiment is not very good even though the spherical calculation correctly predicts that the slope of the dependence $\delta r_p^2(A)$ is about half of the slope expected from the simple relation $R = r_0 A^{1/3}$. This means that, on average, the neutron-proton interaction we use has the correct magnitude.

Next, the equilibrium deformation for the lighter cesium isotopes is included (open squares), leading to a much better agreement. Further improvement is achieved when the effect of zero-point quadrupole vibrational motion is taken into account. It is well known that the mean square radius of a vibrating nucleus is increased by [22]

$$\langle r^2 \rangle_\beta = \langle r^2 \rangle_0 \left(1 + \frac{5}{4\pi} \langle \beta^2 \rangle \right). \quad (17)$$

We include this effect of the shape fluctuations using the quantities $\langle \beta^2 \rangle$ extracted from the measured transition matrix elements $B(E2, 0^+ \rightarrow 2^+)$ and the relation

$$\langle \beta^2 \rangle = B(E2, 0^+ \rightarrow 2^+) [3ZR_0^2/4\pi]^{-2}. \quad (18)$$

We take the average $B(E2)$ of the corresponding Xe and Ba isotopes with neutron numbers $N = 78$ –84 and correct the radii of ^{133}Cs – ^{139}Cs accordingly, as shown in Figs. 2 and 3. Thus, further improvement in the comparison with the measured isotope shifts results. [For $N = 84$ the $B(E2)$ values are not known. We use instead the empirical relation between the energy of the lowest 2^+ state and the deformation parameter $B(E2)$ [23].] This correction results in changes in r^2 of 0.2124 fm² in ^{133}Cs , 0.1325 fm² in ^{135}Cs , 0.0724 fm² in ^{137}Cs , and 0.1263 fm² in ^{139}Cs .

In a fully consistent calculation, one should make a similar correction for the deformed cesium isotopes as well. Since the corresponding $B(E2)$ values for the vibrational states are not known, and the corrections are expected to be small and thus do not have to be known precisely, we assume that the $B(E2)$ values for the γ and β vibrational states give together 10 Weisskopf units, the same for all deformed cesium isotopes. [With such $B(E2)$ values the correction happens to be numerically the same as in the semimagic ^{137}Cs .] We believe this shortcoming explains the somewhat poorer agreement in the deformed cesium isotopes.

Even though the quadrupole 2^+ states contribute most to the mean square radius via Eq. (17), other vibrational states, e.g., the octupole 3^- and the giant resonances, contribute as well; however, all such states not only have smaller collective amplitudes but, even more importantly, vary more smoothly with the atomic mass (or neutron number) than the 2^+ states, and hence their contribution to the shifts δr^2 should be correspondingly smaller.

Altogether, the error in the shift δr_p^2 is at most 0.2 fm², and appears to be independent of the change in the neutron number ΔN . Thus, for the following considerations we assign an uncertainty in the relative value of δr_p^2 of 0.2 fm². Very little is known experimentally about the moments r_p^4 . Quite conservatively, we assume that the uncertainty in δr_p^4 is $\langle r_p^2 \rangle \Delta r_p^2 \simeq 5 \text{ fm}^4$.

In a recent similar HF calculation of the charge radii of the Pb isotopes using SkM* and SkmIII forces, Tajima *et al.* [24] showed that both SkmIII and SkM* failed to reproduce the experimental charge radii kink across the ^{208}Pb shell closure, even though both forces give excellent agreement with the experimental $\langle r_p^2 \rangle$ on the neutron deficient side. Such a failure to reproduce the charge radii kink is also observed in our calculations; however, it is not a serious problem in our case because there is only

TABLE II. Results of the Hartree-Fock calculations with the SkmIII interactions. The experimental binding energies and isotope shifts $\delta\langle r_p^2 \rangle$ are also listed for comparison. (The binding energies are in MeV, all radial moments in fm.) The experimental isotope shifts are from Ref. [32], normalized to the stable isotope ^{133}Cs .

N	B	B_{HF}	$\delta r_p^2(\text{expt})$	δr_p^2	$\delta r_p^2(\text{sph.})$	δr_p^4	δr_n^2	$\delta r_n^2(\text{sph.})$	δr_n^4
70	1049.98	1047.12	-0.1517	-0.1322	-0.5097	7.670	-0.5484	-1.0265	-24.683
72	1068.25	1065.52	-0.0985	-0.1015	-0.3813	6.023	-0.4141	-0.7592	-18.954
74	1085.66	1083.44	-0.0561	-0.0440	-0.2536	6.317	-0.2526	-0.4991	-11.388
76	1102.37	1100.62	-0.0141	-0.0096	-0.1265	3.117	-0.1096	-0.2461	-5.198
78	1118.52	1118.01	0.0000	0.0000	0.0000	0.000	0.0000	0.0000	0.000
80	1134.24	1134.75	0.0250	0.1254	0.1254	6.530	0.2392	0.2392	14.634
82	1149.27	1153.20	0.0821	0.2508	0.2508	13.124	0.4721	0.4721	29.191
84	1159.57	1161.94	0.3604	0.4120	0.4120	22.346	0.8674	0.8674	59.984

one isotope above the $N = 82$ shell closure in our calculations. Moreover, the calculations of Ref. [24] confirm our estimate of the error in the shift δr_p^2 , even though the isotope shifts are larger in lead than in cesium.

Before turning our attention to the neutron radii, it is worthwhile to make a brief comment about the comparison with *absolute* values of $\langle r_p^2 \rangle$ and $\langle r_p^4 \rangle$. Experimentally, muonic x-ray energies for the stable ^{133}Cs have been fitted by the Fermi distribution with the halfway radius $c = 5.85$ fm, surface thickness $t = 1.82$ fm [25,26], and $\langle r_p^2 \rangle = 23.04$ fm². Such a Fermi distribution gives $\langle r_p^4 \rangle = 673$ fm⁴. Our HF calculation corrected for zero-point vibrational motion with $\langle \beta^2 \rangle = 0.024$, as described above, gives $\langle r_p^2 \rangle_{\text{HF}} = 23.27$ fm² for SkmIII and 22.69 fm² for SkM* interactions, both quite close to the experimental value. The calculated $\langle r_p^4 \rangle$ moments (not corrected for the zero-point motion) are 671(SkmIII), and 652(SkM*) fm⁴. We see, therefore, that the calculation is quite successful in the absolute radii (and even surface thicknesses), in particular for the SkmIII interaction (which also gives the correct ground state spin).

The calculated shifts in the neutron radii δr_n^2 are listed in Tables I (SkM*) and II (SkmIII), and the quantities δr_n^2 corrected for the effect of zero-point vibrational motion are displayed in Fig. 4. Several comments about these are in order. First, the slope of the dependence of $\delta r_n^2(A)$ for spherical configurations is correspondingly steeper than the slope following from $R = r_0 A^{1/3}$. That is obviously a correct result; the combination of a smaller slope in the proton radii and a larger slope in the neutron radii when neutrons are added is necessary to maintain on average the $R = r_0 A^{1/3}$ relation. Second, the HF calculations imply that the proton and neutron distributions have essentially identical deformations. This agrees with the general conclusion about the isoscalar character of low-frequency collective modes in nuclei (see, e.g., Ref. [27]). Thus, we accept this result and do not assign any additional uncertainty to the possible difference in the deformation of protons and neutrons. To quantify this statement, recall that a typical deformation for

cesium is $\beta = \sqrt{\langle \beta^2 \rangle} \approx 0.2$; from Eq. (17) and the requirement $\delta r^2 \leq 0.2$ fm², we find $\delta\beta/\beta \leq 0.3$. Our assumption means, therefore, that the proton and neutron deformations agree to within 30%, a rather mild restriction. Finally, for the same reason, we use the same $B(E2)$ values, and the $\langle \beta^2 \rangle$ extracted from them, to correct the neutron radii using Eq. (17). Assuming all of the above, we assign *identical* uncertainties to the neutron shifts δr_n^2 and the proton shifts δr_p^2 , and similarly to the fourth moments $\delta r_{n,p}^4$.

Very little reliable experimental information on the neutron distribution in nuclei is available. In Ref. [28], data from pionic atoms are analyzed. The corresponding best fit for neutron mean square radii agrees very well with the HF results quoted there. The nearest nucleus to cesium in Ref. [28] is ^{142}Ce . Scaling it with $A^{2/3}$, one arrives at $\langle r_n^2 \rangle = 24.7$ fm² for ^{133}Cs , somewhat larger than our calculated values 23.7 and 24.0 for SkM* and SkmIII, respectively. In Ref. [10], the theoretical neutron density of Brack *et al.* [29] with $\langle r_n^2 \rangle = 23.5$ fm² was used. That value, presumably obtained by interpolation from the values obtained by the HF method using the SkM* interaction, is, not surprisingly, quite close to our calculated values. This limited comparison suggests that the absolute radii $\langle r_n^2 \rangle$ have uncertainties of about 1 fm². The uncertainty in the shifts δr_n^2 should be substantially smaller, and our estimated error of 0.2 fm² does not seem unreasonable.

In Ref. [13] the uncertainty in the integrals $q_{n,p}$ was estimated from the spread of the calculated values with a wide variety of interactions. Some of the interactions employed in [13] give better agreement for known quantities (charge radii, binding energies, etc.) than others. We chose to use only the two most successful interactions. The spread in the calculated shifts $\delta r_{p,n}^2$ for these two interactions is less than our postulated error of 0.2 fm².

In this context it is worthwhile to mention the calculations of Ref. [30]. There, proton and neutron radii for several nuclei were evaluated using the Hartree-Fock method with the SkmIII and SkM* interactions, as in the

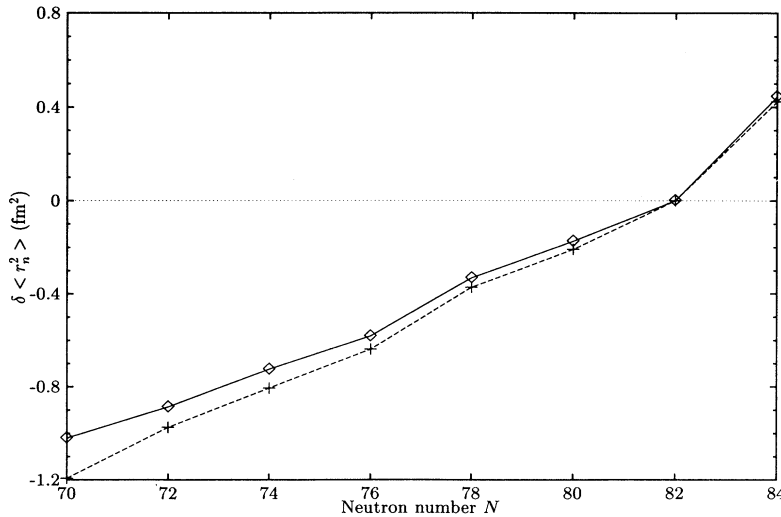


FIG. 4. Calculated changes in the neutron radii $\delta \langle r_n^2 \rangle$ in cesium. The results, corrected for zero-point vibrational motion, and calculated with the SkmIII (\diamond) and SkM* (+) interactions, are shown.

present work, but also within the relativistic mean field approach. The HF results with Skyrme forces seem to agree somewhat better with the empirical data, particularly for the heavier nuclei, and our estimated uncertainty of 1 fm^2 for $\langle r_n^2 \rangle$ in a *single* nucleus agrees with the findings of [30]. (This also supports our choice of the method and interaction.) The only pair of isotopes considered in [30] is ^{116}Sn and ^{124}Sn . The calculated δr_n^2 deviate from the empirical ones by less than 0.3 fm^2 ; i.e., the error is somewhat larger than our assumed error. However, when the experimental uncertainty of about 0.5 fm^2 is taken into account, that discrepancy loses significance.

Pollock *et al.* [13] also argue that the isovector surface term $(\rho_p - \rho_n)\nabla^2(\rho_p - \rho_n)$ in the Skyrme Lagrangian is poorly determined and may affect the neutron skin significantly, without affecting most bulk nuclear properties. We tested this claim by modifying simultaneously the coefficients $B_5 \rightarrow B_5(1+x)$ and $B_6 \rightarrow B_6 - 2B_5x$ in Eq. (12). We find that when we vary x (i.e., the relative strength of the isovector surface term) from $+0.3$ to -0.3 the proton radius $\langle r_p^2 \rangle$ changes indeed very little (about 0.06 fm^2) and the neutron radius changes somewhat more (by about 0.1 fm^2 , still far less than our estimated error for an individual nucleus). The effect on the quantity δr_n^2 is substantially less. At the same time, the binding energy changes by about 5 MeV , more than the largest discrepancy between the theory and experiment. Thus, even a quite substantial change in the isovector surface term will affect the neutron radii (and the difference in neutron radii) by less than our assumed error. At the same time such a modification would clearly spoil the agreement with experiment in the binding energies.

We stressed above that there is essentially no model-independent experimental information on neutron density distributions. Thus, our calculations, and our estimated uncertainties, cannot be verified directly. Instead, we assume that there are no effects which would change the neutron radii substantially, but would not affect the binding energies, proton radii, or other quantities that are well described by the HF method. We are not aware of any such effects, but one has to be aware of this possibility.

IV. ESTIMATED UNCERTAINTIES IN PNC EFFECTS

The nuclear-structure effects are governed by the coefficients $q_{n,p}$, Eq. (5), which in turn involve integrals of the form factors $f(r)$, Eq. (6). The function $f(r)$ is slowly varying over the nuclear volume, and may be accurately approximated by a power series

$$f(r) = 1 + f_2 r^2 + f_4 r^4, \quad (19)$$

and, therefore,

$$q_{n,p} = 1 + f_2 \langle r_{n,p}^2 \rangle + f_4 \langle r_{n,p}^4 \rangle. \quad (20)$$

For a sharp nuclear surface density distribution, the only relevant parameter is the nuclear radius R and $\langle r^{2n} \rangle = 3/(2n+3)R^{2n}$. Using the experimental $\langle r^2 \rangle = 23.04 \text{ fm}^2$ for ^{133}Cs [25], we find from Eq. (6)

$$f(r) \simeq 1 - 2.10 \times 10^{-3} r^2 + 1.09 \times 10^{-5} r^4, \quad (21)$$

where the distance is measured in fermis. However, as pointed out above, the analytic expansion, Eq. (6), is unsuitable at the intended level of accuracy. So, instead, we solve numerically the Dirac equation for the $s_{1/2}$ and $p_{1/2}$ bound electron states in the field of the finite size diffuse surface nucleus, we obtain by fitting the coefficients $f_2(f_4)$ of -2.31×10^{-3} (1.21×10^{-5}) when we use the standard surface thickness parameter $t = 2.25 \text{ fm}$, and -2.267×10^{-3} (1.157×10^{-5}) when we use the surface thickness $t = 1.82 \text{ fm}$ adjusted so that the nuclear density parametrized by the two-parameter Fermi distribution resembles as closely as possible the Hartree-Fock charge density in ^{133}Cs . Also, we make sure that the expansion, Eq. (19), is accurate over the whole nuclear volume, and that it is sufficient to use only the r^2 and r^4 terms in it.

The expansion coefficients f_2, f_4 depend, primarily, on the mean square charge radius. To take this dependence into account, we use for ^{133}Cs the f_2 and f_4 above, and for the other isotopes, we use the same surface thickness parameter ($t = 1.82 \text{ fm}$) as determined by the Hartree-Fock calculation in ^{133}Cs and adjust the halfway radius in such a way that the experimental $\langle r_p^2 \rangle$ are correctly reproduced.

It is easy now to evaluate the uncertainty in the factors $q_{n,p}$ given the coefficients f_2, f_4 and our estimates of the uncertainties in $\langle r^2 \rangle$ and $\langle r^4 \rangle$. Substituting the corresponding values, we find that the uncertainty is $\delta q_{n,p} = 4.6 \times 10^{-4}$, caused almost entirely by the uncertainty in the mean square radii $\langle r_{n,p}^2 \rangle$. This uncertainty represents about 1% of the deviations of $q_{n,p}$ values from unity.

Before evaluating the nuclear-structure corrections $Q_W^{\text{nuc}}(N, Z)$ we have to consider the effect of the intrinsic nucleon structure. Following [13] we use

$$q_{p,n}^{\text{int}} = \int d^3\mathbf{r} \frac{1}{6} \langle r^2 \rangle_{\text{int},(p,n)}^w f(r) \nabla^2 \rho_{p,n} / Q_{p,n}^w, \quad (22)$$

where $\langle r^2 \rangle_{\text{int}}^w$ are the nucleon weak radii, and $Q_{p,n}^w$ are the nucleon weak charges. Neglecting the “strangeness radius” of the nucleon, and using the fitted two-parameter Fermi density distribution, we find

$$q_p^{\text{int}} = -0.00290, \quad q_n^{\text{int}} = -0.00102, \quad (23)$$

very close to the sharp nuclear surface values of Pollock *et al.* [13]. The above intrinsic nucleon-structure corrections are small, but not negligible. More importantly, they are independent of the nuclear structure, and cancel out in the differences $\Delta q_{n,p}$.

The quantities $100(q_n - 1)$ and $100(q_p - 1)$ are listed in Table III for all cesium isotopes and for the two Skyrme interactions we consider. One can see that they vary by about 4% for neutrons and are essentially constant for protons when the neutron number increases from $N = 70$ to 84. The variation with N is essentially identical for the two forces, while the small difference between the $q_{n,p}$ values calculated with the two forces reflects the difference in the *absolute* values of radii for the two interactions.

TABLE III. The radiatively corrected weak charges $Q_W(N, Z)$, nuclear-structure corrections $Q_W^{\text{nuc}}(N, Z)$, and the quantities $q_n - 1$, $q_p - 1$ (the factors $q_{p,n} - 1$ contain the intrinsic nucleon-structure correction, and are multiplied by 100 for easier display) calculated with the SkM* and SkmIII interactions, and with the vibrational corrections described in the text.

N	$Q_W(N, Z)$	$Q_W^{\text{nuc}}(N, Z)$	SkM*		$Q_W^{\text{nuc}}(N, Z)$	SkmIII	
			$q_n - 1$	$q_p - 1$		$q_n - 1$	$q_p - 1$
70	-65.312	2.967	-4.55	-4.64	3.015	-4.62	-4.74
72	-67.283	3.077	-4.58	-4.64	3.118	-4.64	-4.74
74	-69.254	3.184	-4.60	-4.64	3.225	-4.66	-4.75
76	-71.226	3.291	-4.62	-4.64	3.330	-4.68	-4.75
78	-73.197	3.422	-4.68	-4.68	3.458	-4.73	-4.79
80	-75.169	3.528	-4.69	-4.67	3.564	-4.74	-4.79
82	-77.140	3.638	-4.71	-4.68	3.669	-4.76	-4.79
84	-79.112	3.745	-4.73	-4.66	3.780	-4.78	-4.78

The weak charges $Q_W(N, Z)$ and the nuclear-structure corrections $Q_W^{\text{nuc}}(N, Z)$ in Table III are radiatively corrected. Thus, instead of the formulas (8) and (9) we use

$$Q_W(N, Z) = 0.9857[-N + Z(1 - 4.012\bar{x})] \times (1.0 + 0.00782T), \quad (24)$$

$$\bar{x} = 0.2323 + 0.00365S - 0.00261T,$$

following [2]. Here S is the parameter characterizing the isospin-conserving “new” quantum loop corrections, and T characterizes the isospin-breaking corrections [31]. Also,

$$Q_W^{\text{nuc}}(N, Z) = 0.9857 \times [-N(q_n - 1) + Z(1 - 4.012\bar{x})(q_p - 1)]. \quad (25)$$

These quantities, evaluated for $S = T = 0$, are shown in Table III. The assumed uncertainty in the shifts of the mean square radii, and consequently in the changes in factors $q_{n,p}$, results in the relative uncertainty $\delta Q_W/Q_W$ of 5×10^{-4} . That uncertainty, therefore, represents within the nuclear model we use the “ultimate” nuclear-structure limitation on the tests of the standard model in the atomic PNC experiments involving several isotopes.

In the atomic PNC experiments involving a *single* isotope, the uncertainty in the neutron mean square radius is larger, and 1 fm^2 appears to be a reasonable choice. Thus, from nuclear structure alone, the weak charge in a single isotope has relative uncertainty of about 2.5×10^{-3} , perhaps comparable to the best envisioned measurements, but considerably smaller than the present uncertainty associated with the *atomic* structure. (The 5 times larger uncertainty 2.5×10^{-3} for a single isotope, as opposed to the uncertainty 5×10^{-4} in the previous paragraph for a series of isotopes, is a consequence of the 5 times larger *absolute* uncertainty in $\langle r_n^2 \rangle$ as opposed to the uncertainty in the shift δr_n^2 .)

Suppose now that, in an experiment involving several cesium isotopes, one is able to determine the ratio

$$R(N', N) = \frac{Q_W(N', Z) + Q_W^{\text{nuc}}(N', Z)}{Q_W(N, Z) + Q_W^{\text{nuc}}(N, Z)} \quad (26)$$

with some relative uncertainty $\delta R/R$. To a (reasonable) first approximation

$$R(N', N) \approx \frac{Q_W(N', Z)}{Q_W(N, Z)} [1 + q_n(N') - q_n(N)]. \quad (27)$$

Thus, we see that nuclear structure contributes to the uncertainty of R at the level of roughly 7×10^{-4} , where we added the individual errors in quadrature. This uncertainty is much smaller than the anticipated experimental error.

In such a measurement, therefore, the uncertainty in \bar{x} will be

$$\frac{\delta \bar{x}}{\bar{x}} \approx \frac{\delta R}{R} \frac{NN'}{Z\Delta N} \approx 8 \frac{\delta R}{R} \quad (28)$$

(see also [2,13]), where the last factor is evaluated for $N', N = 70, 84$. The above equation illustrates the obvious advantage of using isotopes with large ΔN . Also, by performing the measurement with several isotope pairs, one can further decrease the uncertainty $\delta \bar{x}$.

When considering restrictions (or determination) of the parameters S and T [31] one has to distinguish the PNC experiments involving a single isotope or several isotopes. In a single isotope the contributions involving T largely cancel, and one is left with sensitivity to S only. On the other hand, for several isotopes, and taking ratios, *both* S and T contribute. The uncertainty in the parameters S and T is determined to good approximation from the relation $\delta \bar{x} = 0.00365\delta S - 0.00261\delta T$, and thus

$$\delta S \approx \frac{\delta R}{R} \frac{NN'}{0.014Z\Delta N}, \quad \delta T \approx \frac{\delta R}{R} \frac{NN'}{0.010Z\Delta N}. \quad (29)$$

In conclusion, we have evaluated the nuclear-structure corrections to the weak charges for a series of cesium isotopes, and estimated their uncertainties. Within the model we used (i.e., the Hartree-Fock method with Skyrme interaction with deformation and zero-point motion corrections added as described above), we concluded that the imperfect knowledge of the neutron distribution in cesium isotopes does not represent in the foreseeable future a limitation on the accuracy with which the standard model could be tested in the atomic PNC experiments.

ACKNOWLEDGMENTS

We would like to thank C. Wieman and D. Vieira whose discussion of the proposed experiments inspired

the work described here, and to S. Pollock for his comments to the manuscript. We would also like to thank P. Bonche and P.-H. Heenen for providing us the original HF code which this work is based upon. This research was performed in part using the Intel Touchstone Delta

System operated by Caltech on behalf of the Concurrent Supercomputing Consortium. This work was supported in part by the U.S. Department of Energy under Contract No. DE-F603-88ER-40397, and by the National Science Foundation, Grant No. PHY90-13248.

-
- [1] P. Langacker, M.-X. Luo, and A. K. Mann, *Rev. Mod. Phys.* **64**, 87 (1992).
 - [2] W. Marciano and J. Rosner, *Phys. Rev. Lett.* **65**, 2963 (1990).
 - [3] V. V. Flambaum, I. B. Khriplovich, and O. P. Sushkov, *Phys. Lett.* **146B**, 367 (1984).
 - [4] W. C. Haxton, E. M. Henley, and M. J. Musolf, *Phys. Rev. Lett.* **63**, 949 (1989).
 - [5] M. C. Noecker, B. P. Masterson, and C. Wieman, *Phys. Rev. Lett.* **61**, 310 (1988).
 - [6] M. A. Bouchiat *et al.*, *Phys. Lett.* **117B**, 358 (1982); **134B**, 463 (1984); *J. Phys. (Paris)* **47**, 1709 (1986).
 - [7] E. D. Commins, *Phys. Scr.* **36**, 468 (1987).
 - [8] V. L. Telegdi, in *Fundamental Symmetries in Nuclei and Particles*, edited by H. Henrikson and P. Vogel (World Scientific, Singapore, 1990).
 - [9] C. Wieman, C. Monroe, and E. A. Cornell, in *Laser Spectroscopy X*, edited by M. Ducloy, E. Jacobino, and G. Camy (World Scientific, Singapore, 1991).
 - [10] S. A. Blundell, W. R. Johnson, and J. Sapirstein, *Phys. Rev. Lett.* **65**, 1411 (1990).
 - [11] V. Dzuba, V. Flambaum, and O. Sushkov, *Phys. Lett.* **141A**, 147 (1989).
 - [12] E. N. Fortson, Y. Pang, and L. Wilets, *Phys. Rev. Lett.* **65**, 2857 (1990).
 - [13] S. J. Pollock, E. N. Fortson, and L. Wilets, *Phys. Rev. C* **46**, 2587 (1992).
 - [14] P. Quentin and H. Flocard, *Annu. Rev. Nucl. Part. Sci.* **28**, 523 (1978).
 - [15] P. Bonche, H. Flocard, P.-H. Heenen, S. J. Krieger, and M. S. Weiss, *Nucl. Phys.* **A443**, 39 (1985).
 - [16] D. Vautherin and D. M. Brink, *Phys. Rev. C* **5**, 626 (1972).
 - [17] M. Beiner, H. Flocard, Nguyen Van Giai, and P. Quentin, *Nucl. Phys.* **A238**, 29 (1975).
 - [18] J. Bartel, P. Quentin, M. Brack, C. Guet, and H. B. Hakansson, *Nucl. Phys.* **A386**, 79 (1982).
 - [19] Y. Engel, D. M. Brink, K. Goeke, S. J. Krieger, and D. Vautherin, *Nucl. Phys.* **A249**, 215 (1975).
 - [20] P. Bonche, H. Flocard, and P.-H. Heenen, *Nucl. Phys.* **A467**, 115 (1987).
 - [21] H. Flocard, P. Quentin, A. K. Kerman, and D. Vautherin, *Nucl. Phys.* **A203**, 433 (1973).
 - [22] A. Bohr and B. R. Mottelson, *Nuclear Structure* (Benjamin, Reading, MA, 1975), Vol. I, p. 164.
 - [23] S. Raman, C. W. Nestor, and K. H. Bhatt, *Phys. Rev. C* **37**, 805 (1988).
 - [24] N. Tajima, P. Bonche, H. Flocard, P.-H. Heenen, and M. S. Weiss, *Nucl. Phys.* **A551**, 434 (1993).
 - [25] R. Engfer *et al.*, *At. Data Nucl. Data Tables* **14**, 509 (1974).
 - [26] W. Y. Lee *et al.*, *Phys. Rev. Lett.* **23**, 648 (1969).
 - [27] A. Bohr and B. R. Mottelson, *Nuclear Structure* (Benjamin, Reading, MA, 1975), Vol. II, p. 383.
 - [28] C. Garcia-Recio, J. Nieves, and E. Oset, *Nucl. Phys.* **A547**, 473 (1992).
 - [29] M. Brack, C. Guet, and H.-B. Hakansson, *Phys. Rep.* **123**, 275 (1975).
 - [30] M. M. Sharma and P. Ring, *Phys. Rev. C* **45**, 2514 (1992).
 - [31] M. E. Peskin and T. Takeuchi, *Phys. Rev. Lett.* **65**, 964 (1990).
 - [32] C. Thibault *et al.*, *Nucl. Phys.* **A367**, 1 (1981).